

# VLASOV-FOKKER-PLANCK SIMULATIONS OF PASSIVE HIGHER-HARMONIC CAVITY EFFECTS IN ALS-U\*

G. Bassi<sup>†</sup>, Brookhaven National Laboratory, Upton, USA

## Abstract

We discuss numerical simulations of the Vlasov-Fokker-Planck equation to model passive higher-harmonic cavity (HHC) effects with parameters of the Advanced Light Source Upgrade (ALS-U). The numerical results, obtained with the SPACE code, are compared with a modal analysis of the coupled-bunch instability theory.

## INTRODUCTION

The option to reutilize the existing Advanced Light Source (ALS) normal conducting higher-harmonic cavities (HHCs) for the ALS Upgrade (ALS-U) is discussed in [1]. Optimal and stable conditions for bunch lengthening are met with one cavity and  $R_H = 1.35 \text{ M}\Omega$ , however the power loss  $P = 12.6 \text{ kW}$  exceeds the cavity limit ( $\sim 5 \text{ kW}$ ). Reusing two of the ALS 3rd-harmonic cavities, whose shunt impedance is  $R_H = 1.7 \text{ M}\Omega$ , the power loss per cavity is  $P = 5.1 \text{ kW}$ , within the cavity limit. However, the two ALS HHC system is shown to be unstable, with the longitudinal coupled-bunch mode  $\mu = 1$  exhibiting a fast growth [1]. Besides considering a newly designed HHC system, in [1] it is suggested that the addition of the third ALS HHC in bunch-shortening mode might be a solution to stabilize the HHC system.

Table 1: ALS-U v20r Lattice Parameters

	Symbol	Value	Unit
Ring circumference	$C$	196.5	m
Revolution frequency	$\omega_0/2\pi$	1.526	MHz
Beam energy	$E_0$	2	GeV
Average current	$I_0$	500	mA
Momentum compaction	$\alpha$	2.11	
Natural energy spread	$\sigma_\delta$	0.943	
Energy loss per turn	$U_0$	0.217	MeV
Synchronous phase (no HHCs)	$\phi_1$	158.784	deg
Harmonic number	$h$	328	
Main rf cavity frequency	$\omega_1/2\pi$	500.417	MHz
3 <sup>rd</sup> -harmonic frequency	$\omega_3/2\pi$	1501.251	MHz
Main cavity voltage	$V_1$	0.6	MV
Natural rms bunch length	$\sigma_{z0}$	3.54	mm
Synchrotron tune (no HHCs)	$\nu_{s0}$	1.75	
Synchrotron freq. (no HHCs)	$\omega_{s0}/2\pi$	2.68	kHz
Long. radiation damping	$\tau_z$	14	ms

Table 2: HHC Design Options and Settings

Optimal HHC			
	Symbol	Value	Unit
HHC shunt impedance	$R_H$	1.35	M $\Omega$
HHC quality factor	$Q_H$	20000	
HHC tuning angle	$\psi$	1.419/81.3	rad/deg
HHC resonance frequency	$\omega_R/2\pi$	1501.496	MHz
HHC tuning	$\Delta\omega_R/2\pi$	245	kHz
HHC power loss	$P$	12.6	kW
Rms bunch length	$\sigma_z$	14.24	mm
Two ALS HHCs			
	Symbol	Value	Unit
HHC shunt impedance*	$R_H$	3.4	M $\Omega$
HHC quality factor	$Q_H$	21000	
HHC tuning angle	$\psi$	1.510/86.5	rad/deg
HHC resonance frequency	$\omega_R/2\pi$	1501.835	MHz
HHC detuning frequency	$\Delta\omega_R/2\pi$	584	kHz
HHC power loss*	$P$	5.1	kW
Rms bunch length	$\sigma_z$	14.7	mm

\* Total

Table 3: Main Cavity Parameters

	Symbol	Value	Unit
Main shunt impedance	$R_M$	5	M $\Omega$
Main quality factor	$Q_H$	40000	MHz
Beta coupling	$\beta_c$	3	

## COMPLEX FREQUENCY SHIFT

In [1] the growth-rate of the coupled-bunch mode  $\mu = 1$  is calculated by linearizing the Vlasov equation about the exact numerical solution of the unperturbed particle motion at equilibrium, leading to a dispersion-relation equation, Eq. (22) of [1], which is then solved numerically.

In this paper we follow the mode analysis presented in [2]. Assuming the centroid  $z_m$  (here  $z_m$  should be understood as  $\langle z_m \rangle$ ) of  $M = h$  bunches performing small rigid dipole oscillations, and making for the time evolution of the coupled-bunch mode  $\tilde{z}_\mu$

$$\tilde{z}_\mu(t) = \sum_{m=0}^{M-1} z_m(t) e^{-\frac{i2\pi m\mu}{M}}, \quad (1)$$

$$z_m(t) = \frac{1}{M} \sum_{\mu=0}^{M-1} \tilde{z}_\mu(t) e^{\frac{i2\pi m\mu}{M}}, \quad (2)$$

the following ansatz

$$\tilde{z}_\mu(t) = a_\mu e^{-i(\omega_s + \Omega)t}, \Omega = \omega_r + i\omega_i, \omega_i = \tau^{-1}, \quad (3)$$

\* Work supported by DOE under contract DE-SC0012704

<sup>†</sup> gbassi@bnl.gov

Content from this work may be used under the terms of the CC BY 3.0 licence (© 2019). Any distribution of this work must maintain attribution to the author(s), title of the work, publisher, and DOI

the complex frequency shift  $\Omega$  for the coupled-bunch mode  $\mu = 1$  satisfies

$$\Omega^2 + 2\omega_s\Omega = i \frac{e\alpha I_0}{E_0 T_0} \sum_{p=-\infty}^{+\infty} f_p |\tilde{\lambda}(f_p)|^2 Z_0^{\parallel}(f_p), \quad (4)$$

where  $f_p = (pM + 1)\omega_0$ . In Eq. (4)  $\omega_s$  is the *incoherent* synchrotron frequency modified by the beam loading voltage  $V_b$  induced by stationary symmetric bunches

$$\omega_s^2 = \omega_{s0}^2 - \frac{3e\alpha i_b R_H \omega_{rf} \cos \psi_H \sin \psi_H}{E_0 T_0}, \quad (5)$$

$$V_b(z) = i_b R_H \cos \psi_H \cos(3\omega_{rf} z/c + \psi_H), \quad (6)$$

$$i_b = 2I_0 \tilde{\lambda}(\omega_R). \quad (7)$$

Eq. (4) can be solved for  $\omega_r$  and  $\omega_i$  in the two limit cases a)  $\omega_i \ll \omega_r$  and b)  $\omega_r \ll \omega_i$ , corresponding to an instability with growth rate much smaller and bigger than the frequency shift respectively. It follows that the *coherent* complex frequency shift has the following two set of solutions

a)  $\omega_i \ll \omega_r$

$$\omega_r^2 + 2\omega_s\omega_r = -\frac{e\alpha I_0}{E_0 T_0} \sum_{p=-\infty}^{+\infty} f_p |\tilde{\lambda}(f_p)|^2 \text{Im}Z_0^{\parallel}(f_p),$$

$$\omega_i = \frac{e\alpha I_0}{E_0 T_0 (\omega_r + 2\omega_s)} \sum_{p=-\infty}^{+\infty} f_p |\tilde{\lambda}(f_p)|^2 \text{Re}Z_0^{\parallel}(f_p). \quad (8)$$

b)  $\omega_r \ll \omega_i$

$$\omega_i^2 = \frac{e\alpha I_0}{E_0 T_0} \sum_{p=-\infty}^{+\infty} f_p |\tilde{\lambda}(f_p)|^2 \text{Im}Z_0^{\parallel}(f_p), \quad (9)$$

$$\omega_r + \omega_s = \frac{e\alpha I_0}{2E_0 T_0 \omega_i} \sum_{p=-\infty}^{+\infty} f_p |\tilde{\lambda}(f_p)|^2 \text{Re}Z_0^{\parallel}(f_p).$$

## NUMERICAL SIMULATIONS OF THE VLASOV-FOKKER-PLANCK EQUATION

Numerical simulations of the Vlasov-Fokker-Planck system of equation are performed with the SPACE code [2]. For a numerical study of the performance and stability of the NLS-II passive 3HC system see [3].

The numerical results with parameters of the optimal HHC settings shown in Table 2 confirm the overall stability of the HHC system. However, as already mentioned in the Introduction, the power loss of the HHC exceeds the cavity limit of 5 kW.

In the following discussion we present numerical simulations of the two ALS-U HHC system with parameters shown in Table 2, corresponding to a HHC detuning frequency  $\Delta\omega_R/2\pi = 584$  kHz, giving, under stable condit-

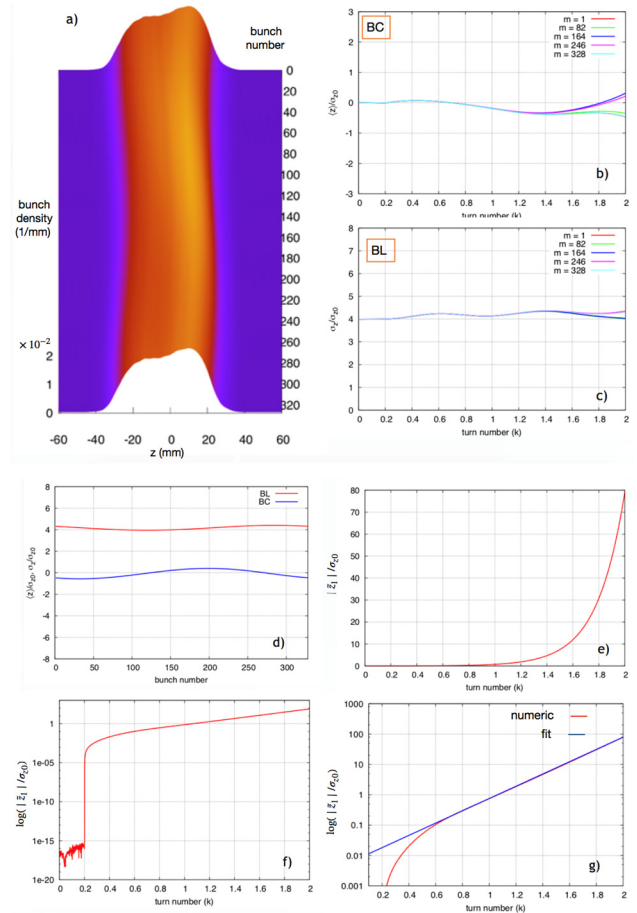


Figure 1: numerical simulations of the two ALS-U HHCs with HHC detuning frequency  $\Delta\omega_R/2\pi = 584$  kHz; a) shows the longitudinal bunch distribution densities after 2000 turns, displaying the unstable coupled-bunch mode  $\mu = 1$ ; (b) and (c) show the time evolution of the bunch centroid and bunch length respectively, for 5 different bunches across the bunch train; (d) shows the bunch centroid and bunch length of all bunch after 2000 turns, clearly displaying the unstable coupled-bunch mode  $\mu = 1$ . The time evolution of the modulus of the coupled-bunch mode  $\mu = 1$  normalized to the natural bunch length  $\sigma_{z0}$  is shown in (e-g), in logarithmic scale. In Fig. 1(g) a linear fit to the numerical result gives the growth time  $\tau_{\text{num}} = 0.139$  ms, in good agreement with the analytical result  $\tau_{\text{an}} = 0.131$  ms given by Eq. (9).

ions, a bunch lengthening factor of  $\sim 4$ . The numerical results are discussed in Fig. 1. Figure 1(a) shows the longitudinal bunch distribution densities after 2000 turns, displaying an instability driven by coupled-bunch mode  $\mu = 1$ . Figures 1(b) and (c) show the time evolution of the bunch centroid and bunch length respectively, for 5 different bunches across the bunch train. Figure 1(d) shows the bunch centroid and bunch length of all bunch after 2000 turns, clearly displaying the unstable coupled-bunch mode  $\mu = 1$ .

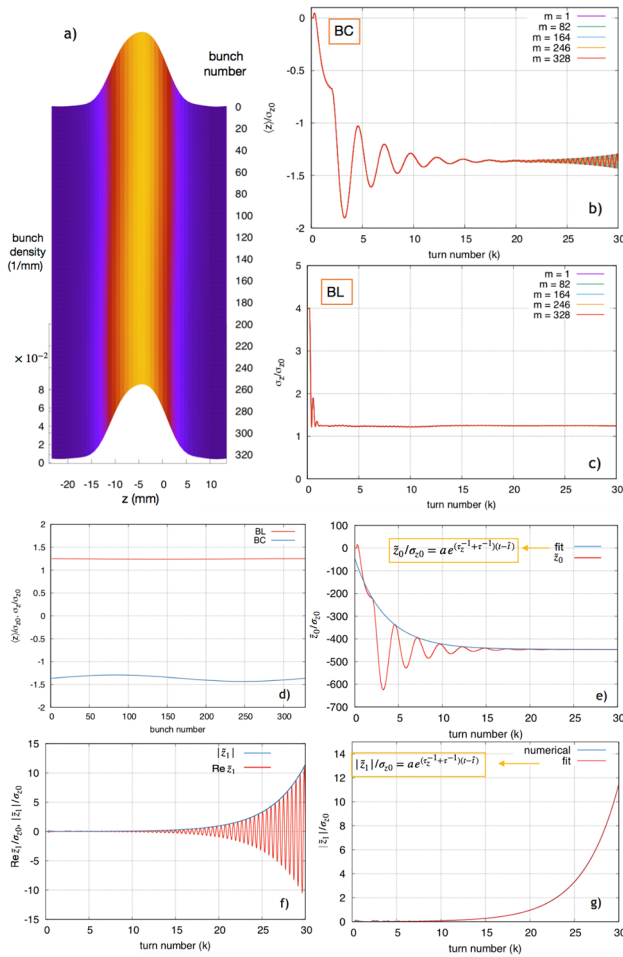


Figure 2: Numerical simulation with HHC detuning frequency of 2000 kHz. (a) shows the longitudinal bunch distribution densities after 30000 turns, displaying the onset of the instability driven by the coupled-bunch mode  $\mu = 1$ ; (b) and (c) show the time evolution of the bunch centroid and bunch length respectively, for 5 different bunches across the bunch train; (d) shows the bunch centroid and bunch length of all bunch after 30000 turns. The time evolution of the coupled-bunch mode  $\mu = 0$  normalized to the natural bunch length  $\sigma_{z0}$  is shown in (e), while (f) and (g) show the time evolution of the unstable coupled-bunch mode  $\mu = 1$ . In (g) an exponential fit to the numerical result to extract the numerical growth time gives  $\tau_{\text{num}} = 2.3$  ms, in good agreement with the analytical result  $\tau_{\text{an}} = 2.4$  ms given by Eq. (8).

The time evolution of the modulus of the coupled-bunch mode  $\mu = 1$  normalized to the natural bunch length  $\sigma_{z0}$  is shown in Fig. 1(e-g) in logarithmic scale. In Fig. 1(g) a linear fit to the numerical result gives the growth time  $\tau_{\text{num}} = 0.139$  ms, in good agreement with the analytical result  $\tau_{\text{an}} = 0.131$  ms given by Eq. (9).

The case corresponding to a HHC detuning frequency  $\Delta\omega_R/2\pi = 2000$  kHz is discussed in Fig. 2, where the numerical calculation of the complex frequency shift shows that the condition of case (b), i.e.  $\omega_i \ll \omega_r$ , is satisfied. To better characterize the development of the instability, the equilibrium distribution has been forced by artificially decreasing the radiation damping time for the first 2000 turns to the value  $\tau = 0.12$  ms. Figure 2(a) shows the longitudinal bunch distribution densities after 30000 turns, displaying the onset of the instability driven by the coupled-bunch mode  $\mu = 1$ . Figure 2(b) and (c) show the time evolution of the bunch centroid and bunch length respectively, for 5 different bunches across the bunch train. Figure 2(d) shows the bunch centroid and bunch length of all bunch after 30000 turns, clearly displaying the unstable coupled-bunch mode  $\mu = 1$ . The time evolution of the coupled-bunch mode  $\mu = 0$  normalized to the natural bunch length  $\sigma_{z0}$  is shown in Fig. 2(e), while Fig. 2(f) and Fig. 2(g) show the time evolution of the unstable coupled-bunch mode  $\mu = 1$ . In Fig. 2(g) an exponential fit to the numerical result to extract the numerical growth time gives  $\tau_{\text{num}} = 2.3$  ms, in good agreement with the analytical result  $\tau_{\text{an}} = 2.4$  ms given by Eq. (8).

## REFERENCES

- [1] M. Venturini, “Passive higher-harmonic rf cavities with general settings and multibunch instabilities in electron storage rings”, *Phys. Rev. Accel. Beams*, vol. 21, 114404, (2018).
- [2] G. Bassi *et al.*, “Self-consistent simulations and analysis of the coupled-bunch instability for arbitrary multibunch configurations”, *Phys. Rev. Accel. Beams*, vol. 19, 024401, (2016).
- [3] G. Bassi and J. Tagger, “Longitudinal Beam Dynamics With a Higher-Harmonic Cavity for Bunch Lengthening”, in *Proc. 13th International Computational Accelerator Physics Conference (ICAP'18)*, Key West, Florida, USA, Oct. 2018, pp. 202-208. doi:10.18429/JACoW-ICAP2018-TUPAF12; and submitted to *Int. J. Mod. Phys. A (IJMP)*